A review on thermoelectric cooling parameters and performance

Diana Enescu [a,*], Elena Otilia Virjoghe [b]

[a] Department of Electronics, Telecommunications and Energy, Valahia University of Targoviste, Unirii Avenue 18-20, 130082 Targoviste, Dambovita, Romania
[b] Department of Automatics, Informatics and Electrical Engineering, Valahia University of Targoviste, 130082 Targoviste, Dambovita, Romania

ARTICLE INFO

ABSTRACT

This paper deals with a review of the main research aspects concerning the formulation of the parameters indicating the characteristics and performance of thermoelectric cooling devices, with particular reference to a number of recent publications. The specific aspects addressed include some practical considerations referring to the thermoelectric figure of merit, the characterization of the cooling capacity, and the assessment of the coefficient of performance (COP). The contribution of this paper starts by categorizing the topics addressed by recent review papers, showing that these reviews generally had a wide focus and provided little specific details on thermoelectric cooling parameters and performance. Then, the dimensionless thermoelectric figure of merit is addressed by focusing on its conventional and modified definitions and indicating the values obtained for different thermoelectric cooling materials. Furthermore, the expressions of the cooling capacity for single-stage and multi-stage thermoelectric coolers are reviewed. Concerning the COP, its dedicated expressions are constructed starting from the classical formulation and introducing additional factors or modifications in order to take into account the Thomson effect, the dependence on temperature of the thermoelectric materials, and the effects of the electrical contact resistance, thermal resistance, thermoelement length and current. Finally, on the basis of the indications taken from the literature, further considerations are included on the COP values found in thermoelectric cooling applications, as well as on how to obtain COP improvements.

© 2014 Elsevier Ltd. All rights reserved.

Contents

---

* Corresponding author. Tel./fax: +40 245217683.
  E-mail addresses: denescu@valahia.ro, enescudiana@yahoo.com (D. Enescu).

1. Introduction

The thermoelectric devices used in thermoelectric refrigeration (or thermoelectric coolers) are based on the Peltier effect to convert electrical energy into a temperature gradient [1]. A conventional thermoelectric cooler is composed of a number of N-type and P-type semiconductor junctions connected electrically in series by metallic interconnects (conducting strips, in general made of copper) and thermally in parallel, forming a single-stage cooler [2]. If a low-voltage DC power source is applied to a thermoelectric cooler, heat is transferred from one side of the thermoelectric cooler to the other side. Therefore, one face of the thermoelectric cooler is cooled and the opposite face is heated.

Fig. 1 depicts a thermoelectric cooling module considered as a thermoelectric refrigerator, in which the electrical current flows from the N-type element to the P-type element [3]. The temperature T_c of the cold junction decreases and the heat is transferred from the environment to the cold junction at a lower temperature. This process happens when the transport electrons pass from a low energy level inside the P-type element to a high energy level inside the N-type element through the cold junction. At the same time, the transport electrons carry the absorbed heat to the hot junction which is at temperature T_h. This heat is dissipated in the heat sink, whilst the electrons return at a lower energy level in the P-type semiconductor (the Peltier effect). If there is a temperature difference between the cold junction and hot junction of N-type and P-type thermoelements, a voltage (called Seebeck voltage) directly proportional to the temperature difference is generated [4,5]. The other parameters appearing in Fig. 1 are introduced in Section 3.2.

The quality of a thermoelectric cooler depends on parameters such as the electric current applied at the couple of N-type and P-type thermoelements, the temperatures of the hot and cold sides, the electrical contact resistance between the cold side and the surface of the device, the thermal and electrical conductivities of the thermoelement, and the thermal resistance of the heat sink on the hot side of the thermoelectric cooler [6]. The number of

thermoelements in a thermoelectric module mainly depends on the required cooling capacity and the maximum electric current [7].

The characteristics and performance of a thermoelectric refrigerator are described by parameters like the figure of merit, the cooling capacity, and the coefficient of performance [4]. This review is specifically focused on these parameters, addressing the concepts in a different way with respect to various review papers appearing on thermoelectric cooling in the past years. Specific aspects such as thermoelectric cooling system design, experimental assessment, numerical analysis and simulation are outside the scope of this review.

The remainder of this paper is organized as follows. Section 2 presents a synthetic overview of recent review papers dedicated to aspects relevant to thermoelectric materials, applications and parameters. Section 3 recalls the basic definitions of figure of merit, cooling capacity, and coefficient of performance. Section 4 addresses some analytical formulations and experimental results referring to the thermoelectric figure of merit. Section 5 presents an assessment of the relevant concepts and literature concerning the cooling capacity. Section 6 deals with the coefficient of performance, starting from its classical expression and introducing specific formulations including the impact of the Thomson effect, the dependence on temperature of the characteristics of the materials, the effect of electrical contact resistances and thermal resistances on the *COP*, with some indications on *COP* improvement. The last section contains the concluding remarks.

2. Overview of recent literature reviews

A summary of recent review papers is provided in Table 1. The relevant topics addressed are categorized into general aspects, applications and parameters, to show that generally these reviews had a wider scope and dedicated a relatively limited space to the details referring to thermoelectric cooling parameters and formulations of the performance indicators.

2.1. Reviews of thermoelectric materials

The first section of topics addressed in some review papers concerns the thermoelectric materials. A related contribution is found in [8], providing specific insights into the development of complex high-efficiency materials. Bell [9] addresses the characteristics of the thermoelectric materials and their potential to be used in various applications for power generation and in households, depending on the average *ZT* value that can be reached, and on the possibility of replacing with thermoelectric systems the cooling systems using cooling agents with high greenhouse gas impact. Tassou et al. [10] review the technologies for food refrigeration, focusing in part on thermoelectric refrigeration. Brown and Domanski [11] review several technologies, with sorption cooling, desiccant cooling, magnetic cooling, thermoacoustic cooling, thermoelectric cooling, and transcritical CO_2 cycle being discussed in some detail. The potential of each technology to reach market viability and compete with other equipment for cooling in the next twenty-year period is addressed. Recent
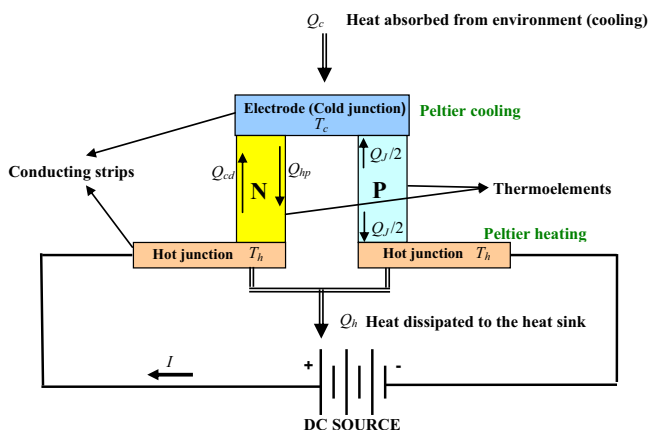

Fig. 1. Scheme of a thermoelectric refrigerator.

Nomenclature

Acronyms

COP	coefficient of performance
DC	direct current
PCM	phase change material
PV	photovoltaic

Symbols

k	thermal conductivity [W/m K]
l	thermoelement length [m]
n	electrical resistivity ratio [m]
p	pairs of semiconductors
q	cooling capacity per unit area [W/m^2]
r	contact resistance per unit area [Ω/m^2]
x	linear coordinate [m]
y	thickness of the contact layers [m]
z	figure of merit of the thermoelectric materials [K^{-1}]
B	normalized temperature dependence of electrical resistivity [K^{-1}]
I	electric current [A]
K	thermal conductance [W/K]
M	number of stages of a module
N	number of thermoelements
P_e	electrical power [W]
Q	heat flux [W]
Q_c	cooling capacity [W]
R	thermal resistance [K/W]
R_e	electrical resistance [Ω]
S	cross-section [m^2]
T	absolute temperature [K]
$\overline{T}$	average temperature [K]
Z	thermoelectric figure of merit [K^{-1}]

ZT	dimensionless figure of merit
ΔT	temperature difference [K]
∇T	thermal gradient [K]
α	Seebeck coefficient [V/K]
χ	thermal conductivity ratio
η	efficiency
ρ	electrical resistivity [$\Omega\,m$]
σ	electrical conductivity [S/m]
τ	Thomson coefficient [V/K]

Subscripts

a	ambient
c	cold side
d	flow from the hot junction to the cold junction
e	electrical
g	heat pumping at the cold junction
h	hot side
i	stage
j	junction
m	module
max	maximum
p	pair
r	relative
v	modified relative
B	normalized temperature dependence
C	Carnot
J	Joule
M	multi-stage module
N	N-type semiconductor
P	P-type semiconductor
ε	electronic component
φ	phonon (or lattice) component

reviews of thermoelectric material types and properties are presented in [12,13].

2.2. Reviews on thermoelectric applications

A number of reviews deal with different types of applications. Simons and Chu [14] discuss a review about thermoelectric cooling and its application to the cooling of electronic equipment. They describe the modern developments and the definition of the main thermoelectric cooling equations, concluding that the thermoelectric coolers are not appropriate for high performance electronic cooling applications due to thermoelectric materials having parameters like figure of merit *Z* and *COP* not good enough. Riffat and Ma [15] review thermoelectric devices and their applications. They describe the importance of the thermoelectric coolers for niche applications (under 25 W) where the cooling demand is limited (e.g., cooler boxes) or the energy cost is not the main issue (e.g., military applications). Furthermore, thermoelectric devices are considered of interest for domestic refrigerators, in spite of their small *COP*, to replace other solutions with higher environmental impact. Xi et al. [16] address thermoelectric refrigeration powered by solar cells, highlighting the relatively small value of the total efficiency (less than 6%) obtained for the total system.

Tassou et al. [10] specify the characteristics and *COP* of prototype domestic refrigerators of large capacity and refrigerator-freezers. A recent review [17] deals with the design and development of new thermoelectric refrigeration and space conditioning systems, presenting the facilities and cost-effectiveness provided

by the thermoelectric cooling system over the conventional cooling system. The authors develop and design an experimental thermoelectric refrigerator with a refrigeration space of 1 l capacity, obtaining a *COP* of 0.1. The thermoelectric cooling systems have an efficiency of 5–15% compared with the efficiency of 40–60% achieved by conventional compression cooling systems.

The advances in household appliances are reviewed in [18], again pointing out that the performance of thermoelectric domestic refrigerator is much lower than that of the conventional vapor compression technology. The result of the single food compartment studied in [19], maintained at 5 °C and obtaining a *COP* of 0.45 at a temperature increase of 19 °C is seen as an interesting application outcome.

An extensive review on the methods about solar refrigeration and cooling systems for the production of cooling energy is provided in [20]. The authors' conclusion is that a liquid desiccant system (consisting of a conditioner and a regenerator) leads to a thermal *COP* higher than for a solid desiccant system (built by melting a thin layer of desiccant material like silica gel on a support structure). Furthermore, it is remarked that solar hybrid cooling systems obtain higher capacity and better thermal *COP*s. Elsheikh et al. [12] discuss a review of thermoelectric renewable energy, mainly focusing on basic parameters that affect thermoelectric efficiency (dimensionless figure of merit *ZT*), applications of thermoelectric devices as coolers (cooling electronic devices, refrigerators and air conditioners) and thermoelectric devices for power generation. Zhao and Tan [13] review thermoelectric cooling applications for refrigeration, electronic cooling, automobile

Table 1
Categorization of recent literature references.

Review paper reference	General aspects		Applications				Sensors	Parameters		Figure of merit
	Cooling technologies and materials	Design and analysis	Electronics equipment	Energy and power generation	Food	Households (refrigeration and air-conditioning)		Coefficient of performance	Cooling capacity	
Simons and Chu [14]	–	–	–	–	–	–	–	–	–	–
Riffat and Ma [15]	–	–	–	–	–	•	•	–	–	–
Riffat and Ma [3]	–	•	•	–	–	–	–	•	–	•
Xi et al. [16]	–	–	•	•	–	•	–	–	–	–
Bell [9]	•	–	•	•	–	–	–	–	–	–
Snyder and Toberer [8]	•	–	–	•	–	–	–	–	–	–
Tassou et al. [10]	•	–	–	–	•	•	–	–	–	–
Bansal et al. [18]	–	–	–	–	–	•	–	–	–	–
Rawat et al. [17]	–	–	–	•	–	•	–	–	–	–
Sarbu and Sebarchievici [20]	•	–	–	–	–	–	–	–	–	–
Brown and Domanski [11]	•	–	•	•	–	•	•	•	–	–
Elsheikh et al. [12]	•	–	•	•	–	•	–	–	–	•
Zhao and Tan [13]	–	•	–	•	–	•	–	–	–	–

cooling, air conditioning and hybrid thermoelectric-photovoltaic modules.

2.3. Reviews on thermoelectric parameters

A few reviews address the specific aspects of the formulation of the main thermoelectric parameters. Riffat and Ma [3] review the *COP* improvement of thermoelectric cooling systems according to the progress of new materials for thermoelectric modules, optimization of module system design and development of the heat exchange efficiency. Their contribution shows that the thermoelement size affects the *COP* of the thermoelectric module, with a large *COP* value obtained for a long thermoelement. It is indicated that a reduction of the contact resistances is essential for improvement of both *COP* and cooling capacity. In addition, design aspects are discussed by specifying new methodologies of analysis for designing high-performance thermoelectric cooling systems. These methodologies include the use of the flow equations for non-dimensional entropy to identify the parameters corresponding with the maximum *COP*, the characterization of the internal and external irreversibilities through a specific parameter, as well as the utilization of multi-stage thermoelectric modules leading to the *COP* improvement for large temperature differences. The contribution presented in [12] recalls the fundamental concepts and reviews a number of recent developments referring to experimental and theoretical progress on the parameters characterizing thermoelectric refrigeration.

3. Basic definitions

3.1. Thermoelectric figure of merit

The *thermoelectric figure of merit Z* indicates if a material is a good thermoelectric cooler. It depends on three material parameters: electrical resistivity ρ (or electrical conductivity $\sigma = 1/\rho$), Seebeck coefficient α and total thermal conductivity k between the cold and hot sides

$$Z = \frac{\alpha^2}{\rho k} = \frac{\alpha^2 \sigma}{k} \qquad (1)$$

Considering the absolute temperature T (which represents the mean temperature between the cold side and hot side of the thermoelectric module), a widely used parameter is the dimensionless product ZT.

An alternative expression of Z takes into account the electrical resistance R of the thermoelements in series and the thermal conductance K of the thermoelements in parallel [21]:

$$Z = \frac{\alpha^2}{RK} \qquad (2)$$

3.2. Cooling capacity

The *cooling capacity* Q_c results from the energy balance at the cold side of the thermoelectric refrigerator:

$$Q_c = \underbrace{\alpha I T_c}_{Q_g} - \underbrace{K \Delta T}_{Q_d} - \underbrace{\frac{1}{2} R_e I^2}_{\frac{1}{2} Q_J} \qquad (3)$$

where

- Q_g is the thermoelectric heat pumping at the cold junction, depending on the Seebeck coefficient α (useful to determine the performance of thermoelements and Peltier elements, characterizes the electronic structure of materials as well as

their thermoelectric properties), the input current I and the temperature of the cold junction T_c.

- Q_d is the heat flow conducted from the hot junction to the cold junction which depends on the thermal conductance K of the thermoelements in parallel, and the temperature difference between hot and cold sides, $\Delta T = T_h - T_c$.
- $Q_J = RI^2$ is the Joule heat, which depends on the electrical resistance R_e of the thermoelements in series and the input current I.

3.3. Coefficient of performance

The *coefficient of performance COP* is the ratio between the cooling capacity Q_c and the electrical power consumption P_e

$$COP = \frac{Q_c}{P_e} \qquad (4)$$

where the electrical power consumption of the thermoelectric refrigerator is given by

$$P_e = \underbrace{R_e I^2}_{Q_J} + \alpha I \Delta T \qquad (5)$$

The electrical power consumption P_e in the thermoelement is the Joule resistance heating plus the work done in driving the current through the thermoelement against the Seebeck voltage caused by the temperature change [22].

4. The thermoelectric figure of merit

4.1. Practical considerations on the dimensionless figure of merit

Starting from the formulation indicated in (1), the dimensionless figure of merit ZT is expressed as

$$ZT = \frac{\alpha^2 T}{\rho k} = \frac{\alpha^2 \sigma T}{k} \qquad (6)$$

where

the term $k = k_\varphi + k_\varepsilon$ is the total thermal conductivity, composed of the phonon (or lattice) component k_φ and the electronic component k_ε; the product $\alpha^2 \sigma$ is called the electrical power factor and depends on the Seebeck coefficient α and on the electrical conductivity σ [8].

In practice, ZT represents the efficiency of the N-type and P-type materials which compose a thermoelement. A thermoelectric material having a higher figure of merit ZT is more convenient, as it can carry out higher cooling power or temperature drop.

The value of the figure of merit is about 1 in the thermoelectric cooling/heating modules and about 0.25 in the air-conditioning applications with efficiency similar to the one of a classical system which uses the R-134A cooling agent [9]. The efficiency of the ideal thermoelectric system increases nonlinearly with ZT. To double the efficiency, ZT has to increase to about 2.2, and for obtaining a fourfold increment (to equal the efficiency of the two-phase refrigerants) ZT has to increase to about 9.2 [9]. In order to exhibit comparable performance with respect to the vapor compression chillers, Gauger et al. [23] and Hermes and Barbosa [24] report that ZT has to increase from a value of the order of unity to 3–4. However, even if ZT is relatively low, thermoelectric cooling can be particularly useful in practical applications because it has no moving parts and has low noise. The figure of merit affects both the maximum temperature difference ΔT_{max} that can be achieved and the maximum COP (see Section 6). Moreover, Gupta et al. [25] indicate that the figure of merit of thermoelectric modules can be increased with the Seebeck coefficient, while the cooling capacity of the heat sink becomes narrow.

Ju and Ghosal [26] present a theoretical analysis in order to describe the behavior of thermoelectric microrefrigerators depending on thermal and electrical contact resistances, boundary Seebeck coefficient, and heat sink conductance. Their study is carried out for observing whether the thermal interface resistance has advantageous or disadvantageous effects on the refrigerator performance. They change the conventional definition of the figure of merit by considering the minimum temperature that can be found at the cold junction for given values of COP and temperature increase that would result without the presence of the thermoelectric cooler, obtaining the following modified form:

$$ZT = \frac{\alpha^2 \sigma}{k} \frac{1 + COP}{1 + 2COP} T \qquad (7)$$

4.2. Figure of merit and materials

Many researches about the figure of merit were carried out in the material science domain. The figure of merit of a material depends on its electronic structure [27]. The three classes of materials (metals, semiconductors, and insulators) can be characterized by zero, small and large band gaps, respectively. To optimize the materials or compounds for thermoelectric applications, some key aspects are the maximization of the figure of merit and the optimization of some parameters of the material. In particular, ZT maximization can be achieved through both maximization of the power factor $\alpha^2 \sigma$ and minimization of the thermal conductivity k, as indicated in [28].

Riffat and Ma [3] report in their review that

- bismuth telluride (Bi_2Te_3), which is the best low-temperature thermoelectric material, has a maximum value of $ZT = 1$ [29];
- if ZT is increased to 2 or 3, the thermoelectric cooling device would be competitive with vapor compression cooling systems;
- if ZT is increased to 6, the thermoelectric devices would be able to cool to cryogenic temperature (77 K) from room temperature.

Current thermoelectric devices are considered to be

- inefficient when ZT is about 1;
- able to recover waste heat when $ZT = 2$;
- able to match a refrigerator when $ZT = 4/5$ [9].

Thermoelectric materials with a high figure of merit ($ZT \geq 1$) can be classified as bulk materials and nanostructured materials. These materials have good electrical properties and low thermal conductivities [30]. In order to improve the figure of merit, references [31–34] report some research contributions on some super-lattice and alloys of different materials. Chowdhury et al. [35] have reduced the temperature of a 1300 W/cm^2 'hot spot' on a test chip with about 7.3 °C by combining both high figure of merit ($ZT \geq 2$) of a thermoelectric material and low electrical contact resistivity. In the past years, some improvements of the figure of merit ZT have been made (e.g., $ZT = 2.4$ in the thin film of Bi_2Te_3 and Sb_2Te_3), as reported in [36]. Zheng [27] carried out a comparison of thermoelectric properties of metals, semiconductors and insulators at 300 K, establishing that insulators with a large band gap have the smallest figure of merit ($ZT = 5 \times 10^{-17}$ K^{-1}) in comparison with metals ($ZT = 3 \times 10^{-6}$ K^{-1}) and semiconductors ($ZT = 2 \times 10^{-3}$ K^{-1}).

The figure of merit of a semiconductor material limits the temperature difference between the hot and cold junctions, while

the length-to-area ratio for a N-type and P-type semiconductor material defines the cooling capacity [37]. Further information about strategies for improving thermoelectric efficiency, namely, addressing the figure of merit for thermoelectric performance, can be found in [27].

Conventionally, thermoelectric cooling materials are bulk solid solution alloys of Bi_2Te_3, Bi_2Se_3, and Sb_2Te_3, with the best materials having ZT of about 1.0 [37,38]. The value of ZT can be enhanced by using materials with higher Seebeck coefficient, increased electrical conductivity and reduced thermal conductivity. However, the needed changes of these properties may be in contrast with each other [38]. Guyer [39] and Riffat and Ma [15] specify that the bismuth telluride which is a pseudo-binary alloy $(Bi,Sb)_2(Se,Te)_3$ is one of the most used thermoelectric materials in refrigeration applications, which works in the temperature range $-120\,°C$ to $230\,°C$. Harman et al. [38] observe that, for room cooling, thermoelectric materials are better than bulk $(Bi,Sb)_2(Se,Te)_3$ solid solution alloy material, due to the ZT values in the range of 1.3 to 1.6 at room temperature. Vikhor and Anatychuk [40] present a method for computing the maximum temperature difference ΔT_{max} of segmented coolers. Using two or three sections of materials with optimized parameters, an increment of about 3–4 K in the maximum temperature difference of the thermoelement made of BiTe is obtained, in comparison with the maximum temperature difference ΔT_{max} of the cooler having $Z = 3.2 \times 10^{-3}\,K^{-1}$ at 300 K. This temperature difference rises to 7–8 K in comparison with the maximum temperature difference ΔT_{max} of the thermoelements made of materials having $Z = 2.95 \times 10^{-3}\,K^{-1}$.

5. Characterization of the cooling capacity

5.1. Cooling capacity for a single thermoelectric cooler

The expression of the cooling capacity per unit area q, taking into account thermal and electrical contact resistances, depends on the thermoelement length l of the module, as reported in [2,21]

$$q = \frac{Q_c}{S} = \frac{k(\Delta T_{max} - \Delta T)}{l + 2\chi y + (\chi y / COP)} \tag{8}$$

where y is the thickness of the contact layers (see Fig. 2), χ is the ratio between the thermal conductivity of the thermoelements and the thermal conductivity of the contact layers, and $\Delta T_{max} = ZT_c^2/2$ is the maximum temperature difference of a module when the cooling capacity is zero.

In practice, starting from a relatively long thermoelement (e.g., over 1.5 mm) and reducing the thermoelement length, the cooling capacity at first grows until it reaches a maximum value, then it starts decreasing. Furthermore, for long thermoelements the contact resistances have a little effect on the cooling capacity, while for short thermoelements the cooling capacity could change

Fig. 2. Representation of the thermoelectric module with indications of the lengths used.

considerably by improving the contact resistances. A case in which the cooling capacity is doubled for a thermoelement with length of 0.3 mm through dividing by two the thermal contact parameter χ is reported in [2].

In the approach proposed in [41], analytical solutions are provided to express the cooling capacity in function of the junction temperature T_j and of the electric current I, by simplifying the thermal balance equations, for a thermoelectric device and for a thermoelectric module. In the latter case, the expression obtained is as follows:

$$Q_c = \frac{T_j[\alpha_m^2 I^2 R_{h,a} - \alpha_m I - K_m] + K_m T_a + (R_{em} I^2 / 2)(2K_m R_{h,a} - \alpha_m I R_{h,a} + 1)}{(\alpha_m I R_{h,a} - 1)(\alpha_m I R_{j,c} - 1) - K_m(R_{h,a} + R_{j,c})} \tag{9}$$

where N is the number of thermoelements forming the module, S is the cross-section, T_a is the ambient temperature, $R_{j,c}$ is the junction-to-cooler thermal resistance, $R_{h,a}$ is the hot side to ambient thermal resistance, $R_{em} = 2N\rho l/S$ is the electrical resistance of the module, $K_m = 2NkS/l$ is the thermal conductance of the module, and $\alpha_m = 2N\alpha$ is the Seebeck coefficient of the module. The expressions obtained are used to solve the optimization of the thermoelectric cooler performance without requiring an iterative procedure. Results are shown on thermoelectric coolers with different cooling capacity.

Huang et al. [42] develop a novel model to predict the cooling capacity by analyzing the performance of a thermoelectric water-cooling device for electronic equipment. According to their application, integrating a water-cooling device with a thermoelectric cooler increases the cooling performance when the heat load is less than a maximum value (57 W in their case). Gupta et al. [25] specify that with a high Seebeck coefficient, the cooling capacity of the heat sink can be an issue, while the figure of merit of the thermoelectric modules can be increased. They suggest enhancement of the cooling capacity of a thermoelectric cooler by using ultra-thin thermoelectric cooler modules.

5.2. Cooling capacity for multi-stage thermoelectric coolers

When a single-stage thermoelectric cooler is not able to work with the temperature difference needed for the specific application, it is possible to use multi-stage configurations to extend the temperature difference that can be considered [7,43,44]. Studies on the cooling capacity of one- and two-stage thermoelectric micro-coolers without taking into account the Thomson effect are reported in [45], specifying that the techniques of integrated circuit and micro-electromechanical manufacturing are essential for thermoelectric cooling development. To reduce the Joule heat effect and to increase the cooling capacity of a thermoelectric cooler (that is, to improve the cooling performance), the Thomson heat is considered positive. Cheng and Shih [46] obtain the maximization of Q_c and COP by optimizing parameters like the electrical current applied and the number of pairs of thermoelements of each stage. Their approach is to compare the optimal parameters obtained with a method based on genetic algorithm with the parameters resulting from the analytical method.

Yu and Wang [47] carry out the optimization of the maximum COP of the cascaded thermoelectric cooler modules taking into account the maximum cooling capacity Q_c. Their computations indicate that the cascaded unit with three stages obtains an increment of about 35.8% in cooling capacity, compared with a single-stage thermoelectric module. They obtain at the same time an increment of the cooling capacity by increasing the applied electrical current. For a cascade cooler, Goldsmid [7] presents the expression of the cooling rate q_i per unit area for the ith stage, depending on the COP of the ith stage and on the cooling rate per
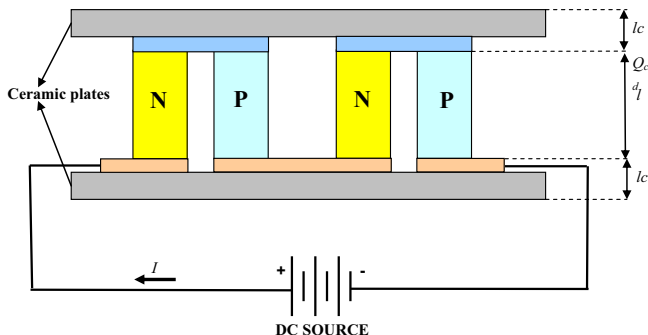
unit area of the Ith stage q_I in connection with the heat source

$$q_i = q_I(1 + COP_I^{-1})(1 + COP_{I-1}^{-1}) \cdots (1 + COP_{I-i}^{-1}) \qquad (10)$$

Also, Goldsmid [7] reports that in a multi-stage cooler each stage considered from the heat source to the heat sink must have a cooling capacity bigger than the one of the previous stage. In fact, each stage rejects both the heat extracted from the previous stage and the Joule heat produced at that stage.

## 6. Assessment of the coefficient of performance (COP)

6.1. Classical expression of the COP

The COP for thermoelectric refrigerators is given by expression (4). The COP values mainly depend on the temperatures at the two sides of the thermoelectric element. This fact is well indicated starting from the definition of the (ideal) Carnot COP, here indicated as COP_C, that considers the temperatures of the hot source T_h and of the cold source T_c:

$$COP_C = \frac{1}{(T_h/T_c) - 1} = \frac{T_c}{T_h - T_c} \qquad (11)$$

The classical expression of the COP, corresponding to the maximum COP [3] used for sizing the thermoelectric element [7,21,47], can be written by introducing a further relative term COP_r that takes into account the figure of merit of the module Z expressed as in (1) and the average temperature $\overline{T} = ((T_h + T_c)/2)$, so that

$$COP = COP_C \, COP_r \qquad (12)$$
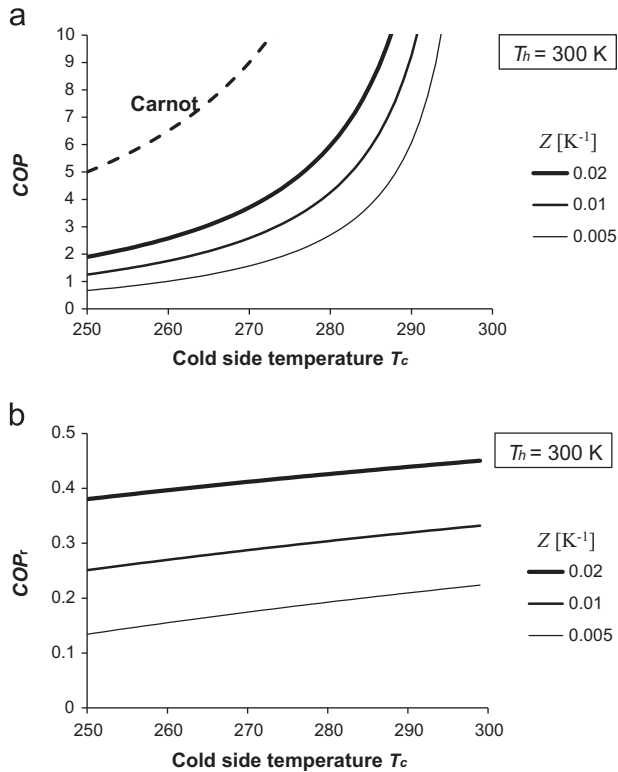
Fig. 3. Values of COP and of the relative component COP_r for different thermoelectric figures of merit Z, at fixed hot side temperature $T_h = 300$ K. (a). COP values and (b) relative component COP_r.

with

$$COP_r = \left(\frac{\sqrt{1 + Z\overline{T}} - (T_h/T_c)}{\sqrt{1 + Z\overline{T}} + 1} \right) \qquad (13)$$

Fig. 3 reports the Carnot COP, the COP and the term COP_r for a thermoelectric device operating at fixed hot side temperature $T_h = 300$ K, in function of the cold side temperature T_c, using different values of Z.

The classical COP expression is simplified, as it neglects the following terms:

- the Thomson effect,
- the dependence on temperature of the characteristics of the materials,
- the effects of the electrical contact resistances, and
- the effects of the thermal resistances.

These simplifications have been addressed by various authors, with the results indicated in the following subsections.

6.2. Impact of the Thomson effect

The *Thomson effect* is given by generation or absorption of a heat quantity in a homogeneous conductor, in which an electric current flows and where there is a temperature gradient. The heat absorption is achieved for one sense of electric current flowing through the conductor, and the heat generation is achieved for the reverse sense of electric current.

Conventionally, the Thomson effect is considered to be

- *positive*, when the hot end has a high voltage and the cold end has a low voltage. Heat is generated when the current flows from the hotter end to the colder end, and heat is absorbed when the current flows from the colder end to the hotter end.
- *negative*, when the hot end has a low voltage and the cold end has a high voltage. Heat is generated when the current flows from the colder end to the hotter end, and heat is absorbed when the current flows from the hotter end to the colder end. Some metals have negative Thomson coefficients (e.g., Co, Bi, Fe, Hg, etc.).

The representative parameter is the Thomson coefficient τ according to which the generated heat flux Q is proportional to the thermal gradient ∇T and to the electric current I which flows through the conductor

$$Q = -\tau I \nabla T \qquad (14)$$

In Rowe [37] an expression of the COP is obtained without taking into account the Thomson effect and considering that the material properties do not depend on the temperature. For thermoelectric elements, the Thomson effect is taken into account in a simplified analytical study in [48], leading to the conclusion that its influence on the COP is about 2%. Huang et al. [49] explain the influence of the Thomson effect by simulating the temperature distribution and the COP for one-stage thermoelectric devices in which the temperatures on the cold and hot sides are considered to be known. In [49], the Thomson effect is also associated with the reduction of the Fourier and Joule heating on the cold surface. The temperature distribution and the cooling power have been analytically studied, observing that both of them are affected by the Thomson effect. Huang et al. [50] indicate that the thermoelectric cooler performance can be improved by increasing the figure of merit of the thermoelectric materials, as well as taking into account the Thomson effect. Fraisse et al. [51] indicate that including the contribution of the Thomson effect as an additive

term in the cooling capacity and electrical power equations is valid only if the temperature dependence of the Seebeck coefficient is taken into account.

The *COP*-dependence on the Thomson effect is addressed in [52], by representing in a bi-dimensional map the *COP* with respect to the dimensionless entropy flux (proportional to the power output or cooling capacity). For a positive Thomson coefficient, the Thomson effect results in reducing the maximum *COP* by about 7.1%, as well as in reducing the cooling capacity by about 7%. Conversely, with a negative Thomson coefficient, both *COP* and cooling capacity can be improved [53].

Yamashita [54] reports that some material properties are not function of the temperature, observing a big influence of temperature-dependent properties for designing high performance of the thermoelectric cooler device. Cherkez [55] describes some possibilities for improving the *COP* of a thermoelectric air conditioner with a combined action of thermoelectric effects and the Joule–Thomson effect. The results obtained show that the *COP* has been increased by 60–70% in comparison with conventional thermoelectric systems (impermeable thermoelement coolers), and by 5–8% in comparison with permeable thermoelements with minor Joule–Thomson effect.

Chen et al. [56] study the distribution of cooling power and the *COP* for three different thermoelectric cooling modules and two temperature differences, taking into account or disregarding the Thomson effect. A big impact of the Thomson effect is observed on the temperature distribution. In particular, the Thomson effect has a greater impact on the P-type element with respect to the N-type element of the thermoelectric cooler. Also, the numerical comparison presented in [56] demonstrates that in the presence of the Thomson effect there is an improvement of *COP* as well as an important increment of the cooling power on the basis of the increment of the number of miniature thermoelectric coolers in a module.

6.3. Dependence on temperature of the characteristics of the materials

The analysis of the dependence on temperature of the characteristics of thermoelectric materials is considered in [54] as an important point in order to obtain a suitable design of thermoelectric devices able to guarantee a relevant performance. Mitrani et al. [57] include the temperature-dependence of the parameters of thermoelectric elements in a simulation-based study. Huang et al. [49] suggest that in the equation of the Seebeck coefficient, the temperature-dependence of the Seebeck coefficient (as well as the Thomson coefficient) can be controlled through a control of the Fermi energy.

6.4. Effects of the electrical contact resistances

The theory reported in [58] concerns the estimation of *COP* on large-dimension thermoelectric modules, in which the electrical and thermal contact resistances are neglected. The same analysis (neglecting the electrical and thermal contact resistances) was made in the case of short thermoelectric modules, but the *COP* results were inadequate. Min and Rowe [21] and Min [59] present an efficient simplified model considering both the thermal and electrical contact resistances for modeling of small-dimension thermoelectric cooling modules advantageous for analysis and optimal design. The improved simplified model presented in [21] shows that the *COP* does not depend on the thermoelement length when the electrical and thermal contact resistances are neglected. By neglecting only the thermal contact resistances and taking into account the electrical resistance of the thermoelement, the figure

of merit *Z* of a single module is written as

$$Z = \frac{zl}{l+n} \tag{15}$$

in which the term n depends on the electrical contact resistivity between the thermoelements and the copper stripes and on the electrical resistivity of the thermoelement materials, while $z = (\alpha^2/\rho k)$ is the figure of merit of the thermoelectric materials employed (which depends on the Seebeck coefficient of the thermoelectric materials, the electrical resistivity ρ and the thermal conductivity of the thermoelement k) and l is the thermoelement length (Fig. 2). As indicated in [21], a typical value for the entry n is 0.1 mm for commercial modules.

By considering only the electrical contact resistance, the *COP* of a single thermoelectric module has the following expression [21]:

$$COP = COP_C \left(\frac{\sqrt{1+(zl/(l+n))\overline{T}} - (T_h/T_c)}{\sqrt{1+(zl/(l+n))\overline{T}} + 1} \right) \tag{16}$$

By applying formula (12) of *COP*, in which COP_r is replaced with the modified term COP_v, and rewriting the term COP_v in such a way to introduce the ratio n/l explicitly, the following expression is obtained:

$$COP = COP_C \, COP_v \tag{17}$$

with

$$COP_v = \left(\frac{\sqrt{1+(z\overline{T}/(1+(n/l)))} - (T_h/T_c)}{\sqrt{1+(z\overline{T}/(1+(n/l)))} + 1} \right) \tag{18}$$

Fig. 4 reports the *COP* and the term COP_v for a thermoelectric device operating at fixed hot side temperature $T_h = 300$ K, in function of the cold side temperature T_c, using values of the ratio n/l consistent with the quantities indicated in [21].
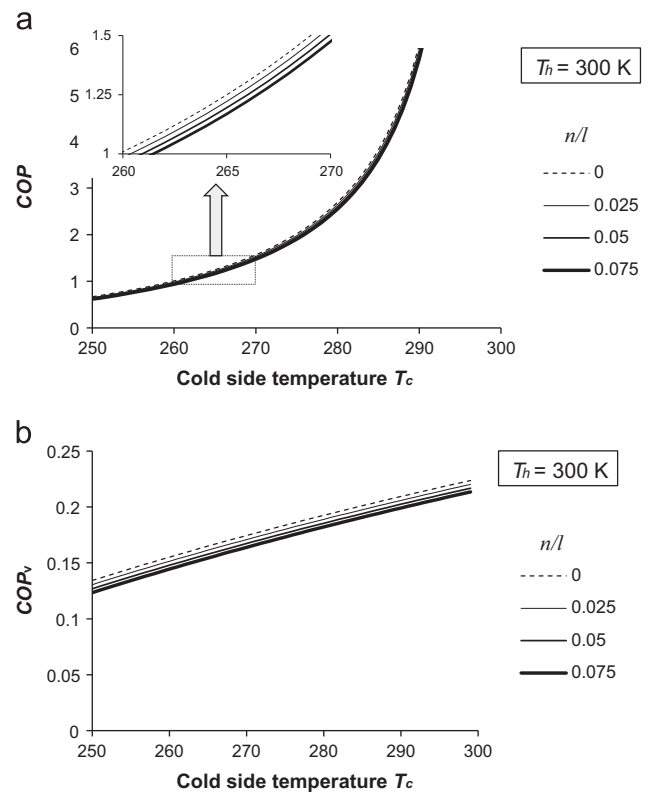

Fig. 4. Values of *COP* and of the modified relative component COP_v for different ratios n/l, at fixed hot side temperature $T_h = 300$ K. (a). *COP* values and (b) relative component COP_v.

According to Rowe [2], the *COP* of the thermoelectric module can be improved up to 60% by reducing the electrical contact resistances. In a recent study, Annapragada et al. [60] illustrate a numerical simulation and experimental assessment of the thermal resistances and of the electrical contact resistivity. The latter has been calculated on the basis of the difference between the power consumption of the thermoelectric modules obtained with and without considering the resistance of the electrical contacts in the model.

A different approach to construct an expression of *COP* taking into account the electrical resistances has been followed in [61]. This approach assumes that the electrical resistivity, the thermal conductivity and the Seebeck coefficient change linearly with the temperature. The resulting formulation of *COP* is obtained:

$$COP = COP_C \, COP_r \, COP_B \tag{19}$$

where COP_r has been defined in (13), and the term COP_B takes into account the normalized temperature-dependence of the electrical resistivity $\rho(T)$ at the average temperature $\overline{T}$, introduced by the term B with the following definition:

$$B = \frac{1}{\rho(T)} \left. \frac{d\rho(T)}{dT} \right|_{T=\overline{T}} \tag{20}$$

The resulting expression of COP_B, elaborated from [61] with notation consistent with the one adopted in this paper, is

$$COP_B = 1 + B\frac{(T_h - T_c)^2}{8T_c} \frac{(1 + (1/\sqrt{1+Z\overline{T}}))}{(\sqrt{1+Z\overline{T}} - (T_h/T_c))} \tag{21}$$

The *COP* of the cooling module is found to depend heavily on the magnitude and sign of the term *B*. Fig. 5 reports the *COP* and the term COP_B for a thermoelectric device operating at fixed hot side temperature $T_h = 300$ K, in function of the cold side temperature T_c, using values of *B* having the order of magnitude indicated in [61].
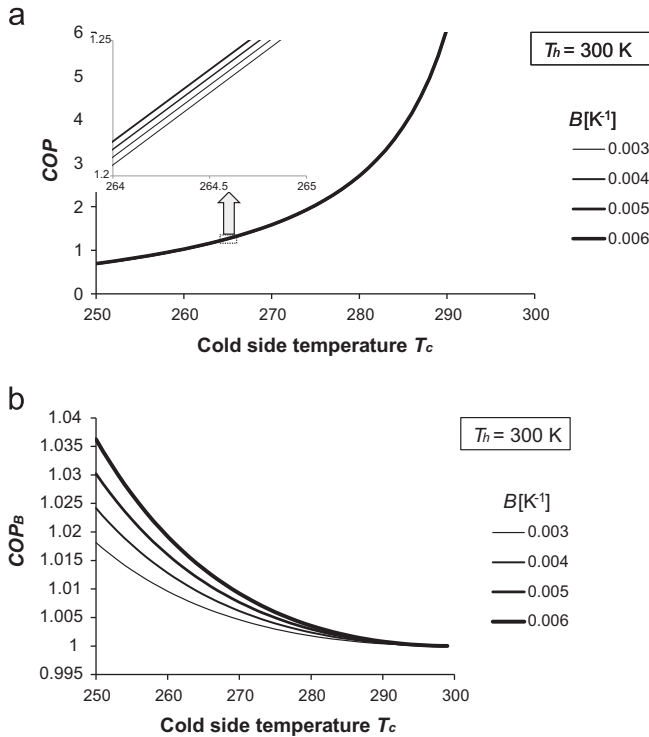
6.5. Effects of the thermal resistances

The thermal resistances are addressed as indicated in [2,21], by taking into account the ratio χ between the thermal conductivity of thermoelements and contact layers, and the thickness of the contact layer *y*, defined in Section 5.1.

On the basis of the changes introduced, it is no longer possible to separate completely the terms due to the thermal resistances from the other terms defining the *COP*. A possible form of the final equation of the *COP* can be written as

$$COP = COP_C \left(\frac{l}{(l+2\chi y)} COP_v - \frac{\chi y}{(l+2\chi y)} \frac{1}{COP_C} \right) \tag{22}$$

In practice, for obtaining a high *COP* a thermoelement has to be relatively long. The effect of temperature-dependence on thermal resistivity is shown in [61] under the hypothesis of linear dependence of thermal resistivity on temperature. Chang et al. [62] develop a model of thermal resistance in order to set up the thermal performance of the thermoelectric air-cooling module. A comparison is carried out between the use of a heat sink, of a thermoelectric module or a combination of the two components. A region of effective operation is identified, in which a combination of the two components has a better performance with respect to using the heat sink only. Pettes et al. [63] adopt the common single-stage thermoelectric refrigerator theory to justify the presence of the thermal and electrical contact resistances. They compute the optimal thermoelement length for maximizing the *COP* for a specified cooling capacity. Therefore, they obtain a reduction by at least 10% of the peak heat removal capability with a reduction of the thermal contact conductance by a factor of ten, and a reduction of the maximum *COP* of at least 50% by increasing the interconnect electrical resistance up to or above ten times the electrical resistance of the legs. Jeong [64] proposes a new one-dimensional analytical model taking into account the contact resistances, obtaining a raise of the optimal current at the same time as the increment of the cooling capacity and the reduction of the temperature difference between the hot and cold sides. A reduction of the optimal thermoelement length with the cooling capacity increase is obtained as well.

6.6. Considerations on the COP dependencies

By considering the simplifications in the *COP* definition through analytical models, the literature has addressed other types of dependencies of the *COP*, mainly through simulations followed by experimental validation. One of the main aspects of the studies, either with analytical or simulation models, is the presence of structures of finite dimension, with the need of setting up appropriate boundary conditions. For example, in [65] the comparison between the numerical and simulation models used leads to a relative error of 7%.

In this respect, it is possible to indicate the following results:

a) *COP dependence on thermoelement length*:
   The conventional theory is valid with long thermoelements, as the *COP* increases for growing thermoelement length [2]. However, for shorter thermoelement length the contact resistance becomes closer to the resistance of the legs, affecting the *COP* more significantly. For example, in an application presented in [2] a high reduction of the *COP* appears when the length of the thermoelement is lower than 1.5 mm.
   The charts of *COP* with respect to thermoelement length for different electrical contact resistances as well as for different thermal contact parameters show an exponential-like variation [21].

Fig. 5. Values of *COP* and of the component COP_B for different values of the normalized temperature-dependence of electrical resistivity *B*, at fixed hot side temperature $T_h = 300$ K. (a) *COP* values and (b) relative component COP_v.

b) *COP dependence on temperature difference and current*:

The *COP* is a function of the temperature difference. In particular, the *COP* increases when the temperature difference decreases. By considering a thermoelectric refrigerator used in household applications, generally the temperature difference has to reach 25–30 K in order to obtain an appropriate cooling effect. In these conditions, the *COP* of the thermoelectric refrigerator can reach values about 0.5–0.7, namely, about 50% of the *COP* of a commercial compressor-type refrigerator [2]. Du and Wen [66] indicate that the maximum *COP* of the thermoelectric elements can be detected when the current is so small as to make temperature difference of about zero. If the current continues to decrease and the temperature difference is less than zero, a reduction of *COP* is observed. The higher values of *COP* can be observed when the temperature difference continues to drop, as well as the head load is added.

Goldsmid [67] proposed the following expression of the electric current corresponding to the maximum *COP*:

$$I_{COP_{max}} = \frac{(T_h - T_c)}{(\sqrt{1 + Z\overline{T}} - 1)} \frac{\alpha_{P,N}}{(R_P + R_N)} \tag{23}$$

where $\overline{T}$ is the average temperature, R_P and R_N are the electrical resistances of the P-type and N-type thermoelement legs, respectively, and $\alpha_{P,N} = \alpha_P - \alpha_N$, in which α_P and α_N are the absolute Seebeck coefficients of N-type and P-type semiconductors, respectively.

The application shown in [68] indicates a *COP* drop on a thermoelectric cooler from 4.5 to 0.3 when temperature differences vary from 5 °C (with current of 1 A) to 30 °C (with current of 5 A), and report some linearized curves of the *COP* with respect to the temperature difference at constant current. However, the relation between the temperature difference and the current is not clearly linear. Pérez-Aparicio et al. [69] analyze the *COP* behavior versus the extracted heat when there is a current increment. At small currents both *COP* and extracted heat increase, while the Peltier effect prevails over the Joule effect. At the maximum current indicated by the manufacturer, the Joule effect becomes prevalent over the Peltier effect and both *COP* and extracted heat decrease. For a given *COP* value, there are two possible current outcomes, one of which is at low current (corresponding to low extracted heat), while the other one is at high current (corresponding to high extracted heat). Du and Wen [66] report an expression of *COP* in which the current appears explicitly, defined by taking into account the Seebeck effect (with Seebeck coefficient α_h at the hot side) and the Fourier effect (with thermal conductivity k) for a thermoelement with p pairs of semiconductors and cross-section S of the semiconductor of P-type, as follows:

$$COP = \frac{Q_c}{2pI\alpha_h T_h - 2pkS\frac{dT}{dx}\big|_{x=h} - Q_c} \tag{24}$$

where the linear coordinate x is defined starting from the hot side ($x = h$).

Rowe [2] and Chen et al. [56] show the *COP*-dependence on the current by the following expression:

$$COP = \frac{\alpha_{P,N}IT_c - (RI^2/2) - k\Delta T}{\alpha_{P,N}I\Delta T + RI^2} \tag{25}$$

which emphasizes that the maximum *COP* does not depend on the number of thermoelectric cooler pairs in a module.

Meng et al. [70] present a model of water-cooling thermoelectric refrigerator, which consists of 127 thermoelectric elements with finned heat exchanger by introducing finite time thermodynamics. Their studies show that the maximum cooling load for

the system analyzed is 2.33 W and the maximum *COP* of the refrigerator is 0.54 when the cooling temperature difference is 10 K. The maximum *COP* decreases by 26% and the maximum cooling load by 34% due to the thermal resistances. The performance of the water-cooling thermoelectric refrigerator can be improved by optimizing the length and cross-section area of the thermoelectric elements. Chen et al. [56] show an application in which the optimal currents with and without the Thomson effect are less than the currents without the temperature difference. They also obtain an increment of the temperature difference due to the influence of the Thomson effect.

6.7. Indications for COP improvement

From the results outlined above, the following indications arise on how to increase the *COP*:

a) Optimize the heat dissipation: for example, Astrain et al. [71] developed a device based on thermosyphon with phase change, aimed at distributing the heat flow referring to the hot side of a Peltier module in the surface of a finned heat sink. Improving heat transfer is a key aspect to increase *COP*. Riffat and Ma [15] indicate that the *COP* of a thermoelectric refrigerator is typically less than 0.5 when operating at temperature difference of about 20 °C. Rowe [2] reports on the existence of thermoelectric refrigeration systems capable of operating with *COP* higher than unity to provide temperature differences of or above 20 °C with respect to the ambient.

b) Reduce the electrical contact and thermal resistances: for example, Bierschenk and Johnson [72] illustrate how optimized configurations of thermoelectric coolers are able to provide a negative thermal resistance in the operation at high *COP*, giving the possibility of extending the limits of air cooling devices for electronics applications. For microprocessor applications, embedded thermoelectric cooling has been introduced in [73] to provide cooling of localized hot spots by using thin thermoelectric devices operating with high heat flux and high *COP*. The need for improving contact resistances in solar thermoelectric refrigerators for increasing the *COP* is indicated in [74].

c) Use new materials, e.g., with negative Thomson effect [53].

d) Use multi-stage modules.

With reference to the latter point, multi-stage thermoelectric cooling modules are useful when usual one-stage thermoelectric cooling modules are not able to provide the required temperature difference. Additional stages increase the temperature difference ΔT between heat source and heat sink, but lead to higher power consumption and to reduction of the thermoelectric system efficiency. Optimized thermoelectric materials are used for cascades of three- and four-stage thermoelectric cooling modules. Generally, the multi-stage modules can be used when the temperature on the cold side is lower than the temperature of a one-stage cooler, as well as when the desired temperature change between the cold and the hot sides cannot be obtained.

In [37] it is reported that the number of stages increases while the minimum temperature on the cold side is reduced, and in [75] it is specified that the *COP* increases at the same time with increasing the number of stages. Chen et al. [43] analyze the performance of a two-stage and a single-stage thermoelectric refrigeration system, obtaining a higher maximum *COP* and smaller maximum rate of refrigeration for the two-stage thermoelectric refrigeration system than for the single-stage one. For a system with M stages, Goldsmid [7] explains the connection between the COP_M of the multi-stage module and the *COP* of one-stage by using the following expression for determining the

COP of the cascade, also linked to (10):

$$1 + COP_M^{-1} = (1 + COP^{-1})^M \qquad (26)$$

from which

$$COP_M = \frac{1}{(1 + COP^{-1})^M - 1} \qquad (27)$$

Yu and Wang [47] propose a multi-stage structure having variable leg length, namely, the leg length decreases from the cold side to the hot side. In the same paper, a procedure for determining the maximum *COP* through numerical calculations is indicated. The result obtained shows that three-stage cascaded units can lead to about 25% *COP* improvement and about 36% improvement in the cooling capacity with respect to the single-stage modules with the same leg length. The maximum *COP* for a single-stage thermo-electric module for an optimum current depends on the figure of merit of the thermoelectric material, as well as on the temperature difference between the hot and cold sides [47]. For a fixed hot side temperature, the maximum *COP* decreases according to an increment of the temperature difference between the hot side and the cold side.

Karimi et al. [44] analyze the performance of multi-stage thermoelectric cooling coolers (a pyramid-type multi-stage thermoelectric cooler with up to 10 stages) for assessing its advantages in comparison with one-stage thermoelectric coolers, taking into account the maximum heat flux and the overall *COP*. They consider the *COP* and the thermal resistance of a heat sink as key parameters in order to obtain analytical formulas for *COP* and heat sink thermal resistance versus electrical current. They observe that the optimal design of a multi-stage thermoelectric cooler is made in accordance with the maximum *COP* and the best heat sink technology. Ma and Yu [76] present a new analytical model of two-stage cascade thermoelectric cooler. According to their study, the maximization of *COP* is obtained for a certain ratio between the leg length at different stages, and a *COP* deterioration is obtained when the temperature of the cold side is high and the ratio of the first-stage leg length to the total leg length is relatively small. Therefore, a two-stage cascade thermoelectric cooler improves the operating temperature difference and is more efficient than a single-stage thermoelectric cooler for the temperatures at which both coolers can operate.

6.8. Notes on the COP of thermoelectric cooling applications

Thermoelectric cooling has various applications for cooling electronic devices [6] and photovoltaic (PV) cells [77] and for refrigerators and air conditioners in the households [78]. Many practical applications have been constructed benefiting from the
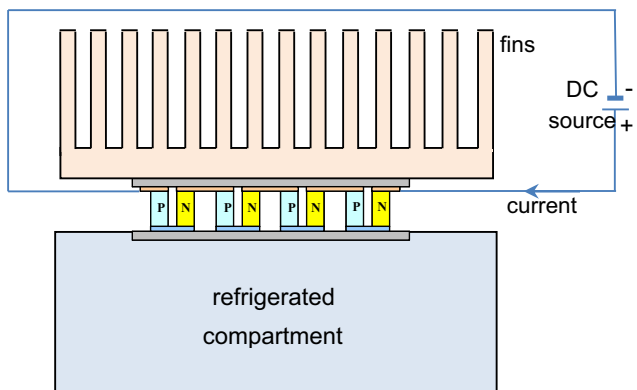

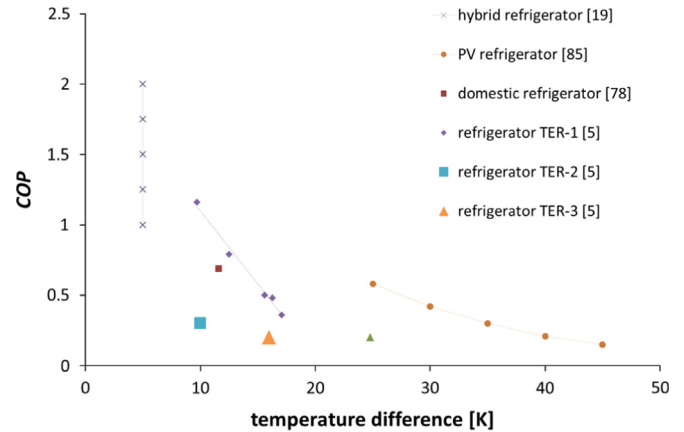**Fig. 6.** Schematic view of a thermoelectric cooling application.

Fig. 7. *COP* values of thermoelectric cooling applications in function of the temperature difference between the hot side and the cold side.

evolution of the technologies in the recent period, with various solutions of different sizes.

A schematic view of a thermoelectric cooling application is shown in Fig. 6, in which the thermoelectric module is mounted on the top of the compartment to be refrigerated, and an additional heat exchanger with fins is placed above the hot side. The system can be integrated with additional forced air circulation through a fan located above the finned heat exchanger. Heat exchanger and fan can also be located inside the refrigerated compartment.

Some notes on the *COP* values found in various applications are presented below, also with reference to the synthetic representation shown in Fig. 7, where the *COP* is represented in function of the temperature difference between the hot side and the cold side.

For micro-cooling applications, the simulations carried out in [79] concern the assessment of the cooling performance of thermoelectric micro-coolers (with thickness of the thermoelectric element from 5 to 20 μm) with the three-dimensional model. A *COP* increasing with the reduction of temperature difference and with the growth of the thickness is obtained. The maximum *COP* is found at a current lower than the one corresponding to the maximum cooling rate. When the temperature difference increases, the current at maximum *COP* becomes large. Thus, the cooling performance depends on the thickness of the thermoelectric element. If the thickness increases, the maximum *COP* increases as well, and the current decreases. Conversely, for thermoelectric elements with reduced thickness, the *COP* becomes relatively low.

An application of a thermoelectric cooler to cooling electronic devices has been presented in [6]. It is reported that the cooling capacity and the *COP* are increasing due to the increment of the cold side temperature and the reduction of the temperature difference between the hot side and the cold side of the thermoelectric cooler. The possibility of obtaining high value of cooling capacity is limited by the cold side temperature and the thermal resistance at the hot side. In this case, microchannel heat sinks are designed to operate at the maximum cooling capacity Q_c of the thermoelectric cooler.

For household applications, Bansal and Martin [78] deal with the cooling performance of a vapor compression system, a thermoelectric refrigeration system and an absorption refrigeration system by comparative analysis, considering a temperature difference of 11.6 °C (that is, a refrigerator compartment temperature of 5 °C for an ambient temperature of 16.6 °C). They obtain the best value of *COP* of 2.59 for the vapor-compression system, followed by thermoelectric refrigeration system with the *COP* of 0.69 (reported in Fig. 7) and the absorption refrigeration system with the *COP* of 0.47. To increase the performance of a conventional vapor
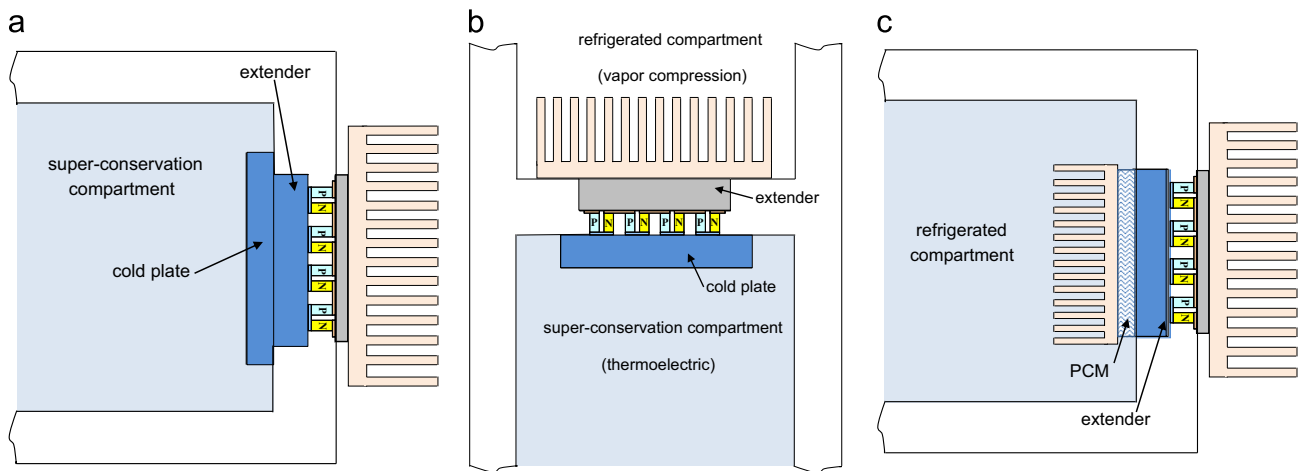
Fig. 8. Schemes of different solutions for thermoelectric refrigeration compartments (the dimensions are not in scale). (a) external hot side, (b) hybrid solution and (c) application with PCM [84].

compression system, Yang et al. [80] propose the utilization of a hybrid thermoelectric system with additional liquid subcooling.

Prototypes of thermoelectric refrigerators have been analyzed in [5], with different types of heat exchangers (called TER-1 with forced convection, TER-2 with forced convection at the cold side and liquid circulation at the hot side, TER-3 with liquid circulation), operating at temperature differences from 9 to 18 K. The different COP values are shown in Fig. 7, corresponding for TER-1 to different input powers, for TER-2 to nominal input power, and for TER-3 estimated from an experimental procedure.

A number of configurations using hybrid refrigerators (combining thermoelectric elements with vapor compression refrigerators) have been analyzed in [19,81]. The main idea is to take advantages both from the high COP that can be obtained from the vapor compression refrigerators and from the temperature controllability of the thermoelectric devices. The different configurations analyzed differ by the position of the thermoelectric devices in the compartments of the refrigerator, with the aim of cooling a specific (super-conservation) compartment of the refrigerator at 0 °C. The cold side of the thermoelement is placed in such a way to be connected with the super-conservation compartment. For the hot side, its connection with the external part of the refrigerator (T_h equal to the ambient temperature, e.g., 25–30 °C, Fig. 8a) was not successful, while its connection with another compartment of the refrigerator cooled with vapor compression at a temperature $T_h=5$ °C (Fig. 8b) provided better results, with COP values ranging from 1 to 2, depending on the thermal resistances of the hot and cold sides, as shown in Fig. 7.

Hermes and Barbosa Jr. [24] made a thermodynamic analysis of Peltier, Stirling and vapor compression portable coolers. From the tests carried out at ambient temperatures around 21 °C the Stirling cooler has the highest $COP \cong 1$, followed by the vapor compression systems (about 1 with reciprocating compressor, and about 0.5 with linear compressor) and by the thermoelectric cooler ($COP \cong 0.2$ for a temperature difference of 24.8 K, indicated in Fig. 7).

Improvements in the performance of thermoelectric refrigerators have been obtained by using two-phase loop thermosyphons [82]. A thermoelectric refrigerator in which the cold side of a Peltier module is in contact with a two-phase and capillary lift thermosyphon, while the hot side is in contact with a two-phase thermosyphon with natural convection has been developed in [83]. For the latter system, the use of the thermosyphons increases of 66% the COP of the thermoelectric refrigerators. In a further application [84], a phase change material (PCM) has been introduced in the refrigeration compartment, between the thermoelectric system and the heat exchanger (Fig. 8c), with the advantage of limiting the reduction of

the internal temperature in the refrigerator compartment when the door is open or after a power supply interruption.

A model of water-cooling thermoelectric refrigerator, which consists of 127 thermoelectric elements with finned heat exchanger, is presented in [70] by introducing finite time thermodynamics. The performance of a multi-purpose thermoelectric refrigerator is analyzed in [85], showing the current, differential temperature and time by controlling the cooling system at ten points. A reduction of the cold side temperature in time is also considered.

For thermoelectric refrigerators powered through solar cells, the COP of the refrigerators is typically not higher than 0.6 [16]. From the experimental analysis carried out in [86], the COP values obtained with $T_c=5$ °C and T_h variable from 30 to 50 °C are shown in Fig. 7. Taking into account the photovoltaic system efficiency η_{PV}, the total efficiency of the system is given by the product of η_{PV} and COP, resulting in values generally lower than 6% [16]. The total efficiency may increase with the enhancement of the photovoltaic system efficiency and with the use of materials with better thermoelectric performance.

For air conditioning applications, Riffat and Qiu [87] report a comparative analysis of three devices for domestic air-conditioning (compression air-conditioner, absorption air-conditioner, and thermoelectric air-conditioner). According to their study, the most efficient one is the vapor compression air-conditioner having the COP of $2.6 \div 3.0$, followed by absorption air-conditioner with the COP of $0.6 \div 0.7$(single effect absorption) and thermoelectric with the COP of $0.38 \div 0.45$. However, the potential interest of using thermoelectric air-conditioners depends on the fact that they work with DC input and as such can be directly connected to sources like photovoltaic cells, fuel cells and in perspective batteries from plug-in electric vehicles. Further advantages of thermoelectric air-conditioners are that their use can reduce the issues due to noise and adoption of ozone-depleting chlorofluorocarbons in vapor compression air-conditioners.

7. Concluding remarks

Thermoelectric cooling is one of the main applications of the thermoelectric devices. This paper has reviewed the formulations of the parameters representing the characteristics and performance of thermoelectric cooling, providing indications on the different formulations of these parameters in order to take into account more detailed effects, and on the values of these parameters found in different applications presented in the recent literature. In particular, on the point of view of the materials,

micro-electronics is a significant field of application, for which the absence of moving parts in thermoelectric devices is very important. Further benefits can be obtained from the development of thermoelectric materials with higher figure of merit, passing from the values of ZT values around unity typical of the best commercial solutions available to higher values (with the maximum experimental ZT value of about 3 at 550 K reported in [88]), as well as from the development of dedicated multi-stage structures providing enhancements in the cooling capacity (e.g., over 35% of improvement for a three-stage module with respect to the single-stage module is indicated in [47]).

Concerning performance aspects, for cooling applications in households conceived in a traditional way (e.g., refrigerators operating with a fixed temperature set point) the thermoelectric devices exhibit COP values typically below 0.5 for temperature differences of 20 K or higher. In this respect, thermoelectric refrigeration is not competitive with alternative solutions such as vapor-compression refrigerators (with COP of about 2.5). However, the interest in the use of thermoelectric refrigerators is increasing because of their useful controllability features. In fact, partial load operation is readily available by changing the electric current. Furthermore, the COP increases when the cooling power is reduced. In this way, solutions in which thermoelectric refrigerators are exploited (as individual equipment or as a part of hybrid solutions with vapor-compression and thermoelectric compartments) become of clear interest to be integrated in a structure for demand-side management when flexible electrical demand is required. The key point is to obtain flexibility in the electrical demand without deteriorating the cooling effect. In this respect, the cooling power variations have to be scheduled in such a way that the temperature inside the refrigeration compartment remains within user-specified boundaries. An additional contribution to this flexibility may come from the introduction of a PCM in the refrigeration system. For example, the test carried out in [84] showed that, for a refrigerator with PCM, after turning the power supply off the internal temperature rose four times more slowly than in the conventional system without PCM, thus improving the performance of thermoelectric refrigeration. The capability of this system to limit the reduction of the internal temperature in particular conditions (e.g., door open or after electrical power supply interruptions) [89], provides additional value to the refrigerator as a flexible electrical load.

Modularity is a further key advantage of thermoelectric devices for many applications. In addition, these devices do not exhibit issues about noise, thus being of interest in many cases in which noise may be a relevant factor, such as air-conditioning in households and in vehicles. Moreover, a key benefit is the possibility of introducing thermoelectric cooling to replace other cooling systems using polluting refrigerants in locations in which the environmental impact is critical.

Solutions providing flexible electrical loads are particularly suitable to be part of the evolving scenario toward the deployment of 'smart' energy systems and buildings [90,91]. In this context, further assets of the thermoelectric systems include their reversible operation as heaters or coolers obtainable by changing the direction of the electrical current. Specific results on the flexibility aspects of demand-side management using thermoelectric cooling devices will be reported in future contributions.

References

[1] Tritt TM. Thermoelectric materials: principles, structure, properties, and applications. Encyclopedia of materials: science and technology. Kidlington, Oxford, UK: Elsevier Science Ltd.; 2002; 1–11.

[2] Rowe DM. Thermoelectrics handbook – macro to nano. Boca Raton (FL): CRC Press Taylor & Francis; 2006.

[3] Riffat SB, Ma XL. Improving the coefficient of performance of thermoelectric cooling systems: a review. Int J Energy Res 2004;28(9):753–68.

[4] Min G, Rowe DM. Peltier device as a generator. CRC handbook of thermoelectric. New York: CRC Press; 1995.

[5] Min G, Rowe DM. Experimental evaluation of prototype thermoelectric domestic-refrigerators. Appl Energy 2006;83:133–52.

[6] Chein R, Huang G. Thermoelectric cooler application in electronic cooling. Appl Therm Eng 2004;24(14–15):2207–17.

[7] Goldsmid JH. Introduction to thermoelectricity. Series in material science. Berlin Heidelberg: Springer; 2010.

[8] Snyder GJ, Toberer ES. Complex thermoelectric materials. Nat Mater 2008;7:105–14.

[9] Bell LE. Cooling, heating, generating power and recovering waste heat with thermoelectric systems. Science 2008;321:1457–61.

[10] Tassou SA, Lewis JS, Ge YT, Hadawey A, Chaer I. A review of emerging technologies for food refrigeration applications. Appl Therm Eng 2010;30: 263–76.

[11] Brown JS, Domanski PA. Review of alternative cooling technologies. Appl Therm Eng 2014;64(1–2):252–62.

[12] Elsheikh MH, Shnawah DA, Sabri MFM, Said SBM, Hassan MH, Bashir MBA, et al. A review on thermoelectric renewable energy: principle parameters that affect their performance. Renew Sustain Energy Rev 2014;30:337–55.

[13] Zhao D, Tan G. A review of thermoelectric cooling: materials, modeling and applications. Appl Therm Eng 2014;66(1–2):15–24.

[14] Simons RE, Chu RC. Application of thermoelectric cooling to electronic equipment: a review and analysis. In: Proceedings of the sixteenth annual IEEE semiconductor thermal measurement and management symposium; 2000. p. 1–9.

[15] Riffat SB, Ma X. Thermoelectrics: a review of present and potential applications. Appl Therm Eng 2003;23:913–35.

[16] Xi H, Luo L, Fraisse G. Development and applications of solar-based thermoelectric technologies. Renew Sustain Energy Rev 2007;11(5):923–36.

[17] Rawat MK, Chattopadhyay H, Neogi S. A review on developments of thermoelectric refrigeration and air conditioning systems: a novel potential green refrigeration and air conditioning technology. Int J Emerg Technol Adv Eng 2013;3(3):362–7.

[18] Bansal P, Vineyard E, Abdelaziz O. Advances in household appliances – a review. Appl Therm Eng 2011;31:3748–60.

[19] Vián JG, Astrain D. Development of a hybrid refrigerator combining thermoelectric and vapor compression technologies. Appl Therm Eng 2009;29 (16):3319–27.

[20] Sarbu I, Sebarchievici C. Review of solar refrigeration and cooling systems. Energy Build 2013;67:286–97.

[21] Min G, Rowe DM. Improved model for calculating the coefficient of performance of a Peltier module. Energy Convers Manag 2000;2(41):163–71.

[22] Parrot JE, Penn AW. The design theory of thermoelectric cooling elements and units. Solid State Electron 1961;3:91–9.

[23] Gauger DC, Shapiro HN, Pate MB. Alternative technologies for refrigeration and air-conditioning applications. United States environmental protection agency. Project summary EPA/600/SR-95/066; 1995.

[24] Hermes CJL, Barbosa Jr JR. Thermodynamic comparison of Peltier, Stirling, and vapor compression. Appl Energy 2012;91:51–8.

[25] Gupta MP, Sayer M, Mukhopadhyay S, Kumar S. Ultrathin thermoelectric devices for on-chip Peltier cooling. IEEE Trans Compon, Packag Man Technol 2011;1(9):1395–405.

[26] Ju YS, Ghoshal U. Study of interface effects in thermoelectric microrefrigerators. J Appl Phys 2000;88(7):4135–9.

[27] Zheng JC. Recent advances on thermoelectric materials. Front Phys China 2008;3(3):269–79.

[28] Zlatic V, Hewson AC. Properties and applications of thermoelectric materials. The search for new materials for thermoelectric devices. In: Proceedings of the NATO advanced research workshop on properties and application of thermoelectric materials B: physics and biophysics. Springer; 2008.

[29] Min G, Rowe DM. Symbiotic application of thermoelectric conversion for fluid preheating/power generation. Energy Convers Manag 2002;43:221–8.

[30] Nolas GS, Poon J, Kanatzidis M. Recent developments in bulk thermoelectric materials. MRS Bull 2006;31(3):199–205.

[31] Hone J, Ellwood I, Muno M, Mizel A, Cohen ML, Zettl A. Thermoelectric power of single-walled carbon nanotubes. Phys Rev Lett 1998;80(5):1042–5.

[32] Hsu KF, Loo S, Guo F, Chen W, Dyck JS, Uher C, et al. Cubic $AgPbmSbTe2+m$: Bulk thermoelectric materials with high figure of merit. Science 2004;303:818–21.

[33] Poudel B, Hao Q, Ma Y, Lan Y, Minnich A, Yu B, et al. High-thermoelectric performance of nanostructured bismuth antimony telluride bulk alloys. Science 2008;320:634–8.

[34] Venkatasubramanian R, Siivola E, Colpitts T, O'Quinn B. Thin film thermoelectric devices with high room-temperature figures of merit. Nature 2001;413:597–602.

[35] Chowdhury I, Prasher R, Lofgreen K, Chrysler G, Narasimhan S, Mahajan R, et al. On chip cooling by superlattice-based thin-film thermoelectrics. Nat Nanotechnol 2009;4:235–8.

[36] Yamashita O, Odahara H, Ochi T, Satou K. Dependence of Seebeck coefficient on a load resistance and energy conversion efficiency in a thermoelectric composite. Mater Res Bull 2007;42:1785–803.

[37] Rowe DM. Handbook of thermoelectric. Introduction. Boca Raton (FL): CRC Press; 1995.

[38] Harman TC, Taylor PJ, Walsh MP, LaForge BE. Quantum dot superlattice thermoelectric materials and devices. Research articles. Science 2002;297: 2229–32.
[39] Guyer EC. Handbook of applied thermal design. New York: McGraw Hill; 1988.
[40] Vikhor LN, Anatychuk LI. Theoretical evaluation of maximum temperature difference in segmented thermoelectric coolers. Appl Therm Eng 2006;26: 1692–6.
[41] Zhang HY. A general approach in evaluating and optimizing thermoelectric coolers. Int J Refrig 2010;33(6):1187–96.
[42] Huang HS, Weng YC, Chang YW, Chen SL, Ke MT. Thermoelectric water-cooling device applied to electronic equipment. Int Commun Heat Mass Transf 2010;37:140–6.
[43] Chen J, Zhou Y, Wang H, Wang JT. Comparison of the optimal performance of single- and two-stage thermoelectric refrigeration systems. Appl Energy 2002;73:285–98.
[44] Karimi G, Culham JR, Kazerouni V. Performance analysis of multi-stage thermoelectric coolers. Int J Refrig 2011;34:2129–35.
[45] Yang R, Chen G. Multistage thermoelectric microcoolers. J Appl Phys 2004;95: 8226–32.
[46] Cheng YH, Shih C. Maximizing the cooling capacity and COP of two-stage thermoelectric coolers through genetic algorithm. Appl Therm Eng 2006;26: 937–47.
[47] Yu J, Wang B. Enhancing the maximum coefficient of performance of thermo-electric cooling modules using internally cascaded thermoelectric couples. Int J Refrig 2009;35:32–9.
[48] Chen J, Yan Z, Wu L. Nonequilibrium thermodynamic analysis of a thermo-electric device. Energy 1997;22(10):979–85.
[49] Huang M, Yen R, Wang A. The influence of the Thomson effect on the performance of a thermoelectric cooler. Int J Heat Mass Transf 2005;48:413–8.
[50] Huang MJ, Chou PK, Lin MC. Thermal and thermal stress analysis of a thin-film thermoelectric cooler under the influence of the Thomson effect. Sens Actuat. A 2006;126:122–8.
[51] Fraisse G, Ramousse J, Sgorlon D, Goupil C. Comparison of different modeling approaches for thermoelectric elements. Energy Convers Manag 2013;65: 351–6.
[52] Chakraborty A, Saha BB, Koyama S, Ng KC. Thermodynamic modelling of a solid state thermoelectric cooling device: temperature–entropy analysis. Int J Heat Mass Transf 2006;49(19–20):3547–54.
[53] Chen J, Yan Z. The influence of Thomson effect on the maximum power output and maximum efficiency of a thermoelectric generator. J Appl Phys 1996;79:8823–8.
[54] Yamashita O. Effect of linear and non-linear components in the temperature dependences of thermoelectric properties on the cooling performance. Appl Energy 2009;86:1746–56.
[55] Cherkez R. Theoretical studies on the efficiency of air conditioner based on permeable thermoelectric converter. Appl Therm Eng 2012;38:7–13.
[56] Chen WH, Liao CY, Hung CI. A numerical study on the performance of miniature thermoelectric cooler affected by Thomson effect. Appl Energy 2012;89:464–73.
[57] Mitrani D, Salazar J, Turó A, García MJ, Chávez JA. One-dimensional modeling of TE devices considering temperature-dependent parameters using SPICE. Microelectron J 2009;40(9):1398–405.
[58] Ioffe AF. Semiconductor thermoelements and thermoelectric cooling. London: Infosearch; 1957.
[59] Min G. Thermoelectric module design theory. In: Rowe DM, editor. Thermo-electric handbook: macro to nano. Boca Raton: CRC Press; 2006.
[60] Annapragada SR, Salamon T, Kolodner P, Hodes M, Garimella SV. Determina-tion of electrical contact resistivity in thermoelectric modules (tems) from module-level measurements. IEEE Trans Compon, Packag Manuf Technol 2012;2(4):668–76.
[61] Yamashita O. Effect of temperature dependence of electrical resistivity on the cooling performance of a single thermoelectric element. Appl Energy 2008;85:1002–14.
[62] Chang YW, Chang CC, Ke MT, Chen SL. Thermoelectric air-cooling module for electronic devices, original research article. Appl Therm Eng 2009;29(13): 2731–7.
[63] Pettes AM, Hodes MS, Goodson KE. Optimized thermoelectric refrigeration in the presence of thermal boundary resistance. IEEE Trans Adv Packag 2009;32:423–30.
[64] Jeong ES. A new approach to optimize thermoelectric cooling modules. Cryogenics 2014;59:38–43.

[65] Astrain D, Vián JG, Albizua J. Computational model for refrigerators based on Peltier effect application. Appl Therm Eng 2005;25(17–18):3149–62.
[66] Du CY, Wen CD. Experimental investigation and numerical analysis for one-stage thermoelectric cooler considering Thomson effect. Int J Heat Mass Transf 2011;54(23–24):4875–84.
[67] Goldsmid JH. Electronic refrigeration. London: Pion; 1986.
[68] Cosnier M, Fraisse G, Luo L. An experimental and numerical study of a thermoelectric air-cooling and air-heating system. Int J Refrig 2008;31 (6):1051–62.
[69] Pérez–Aparicio JL, Palma R, Taylor RL. Finite element analysis and material sensitivity of Peltier thermoelectric cells coolers. Int J Heat Mass Transf 2012;55(1):1363–74.
[70] Meng F, Chen L, Sun F. Performance prediction and irreversibility analysis of a thermoelectric refrigerator with finned heat exchanger. Acta Phys Pol A 2011;120:397–406.
[71] Astrain D, Vián JG, Domínguez M. Increase of COP in the thermoelectric refrigeration by the optimization of heat dissipation. Appl Therm Eng 2003;23 (17):2183–200.
[72] Bierschenk J, Johnson D. Extending the limits of air cooling with thermoelec-trically enhanced heat sinks. In: Proceedings of the ninth intersociety conference on thermal and thermomechanical phenomena in electronic systems, vol. 1; 2004. p. 679–84.
[73] Snyder GJ, Soto M, Alley R, Koester D, Conner B. Hot spot cooling using embedded thermoelectric coolers. In: Proceedings of IEEE twenty-second annual semiconductor thermal measurement and management symposium; 2006. p. 135–43.
[74] Abdul-Wahab SA, Elkamel A, Al-Damkhi AM, Al-Habsi IA, Al-Rubai'ey' HS, Al-Battashi HK, et al. Design and experimental investigation of portable solar thermoelectric refrigerator. Renew Energy 2009;34:30–4.
[75] Nolas GS, Goldsmid HJ, Sharp J. Thermoelectrics: basic principles and new materials developments. New York: Springer; 2001.
[76] Ma M, Yu J. An analysis on a two-stage cascade thermoelectric cooler for electronics cooling applications. Int J Refrig 2014;38:352–7.
[77] Najafi H, Woodbury KA. Optimization of a cooling system based on Peltier effect for photovoltaic cells. Sol Energy 2013;91:152–60.
[78] Bansal PK, Martin A. Comparative study of vapour compression, thermo-electric and absorption refrigerators. Int J Energy Res 2000;24:93–107.
[79] Lee KH, Kim OJ. Analysis on the cooling performance of the thermoelectric micro-cooler. Int J Heat Mass Transf 2007;50(9–10):1982–92.
[80] Yang B, Ahuja H, Tran TN. Thermoelectric technology assessment: application to air conditioning and refrigeration. HVAC&R 2008;14(5):635–53.
[81] Astrain D, Martínez A, Rodríguez A. Improvement of a thermoelectric and vapour compression hybrid refrigerator. Appl Therm Eng 2012;39:140–50.
[82] Lee JS, Rhi SH, Kim CN, Lee Y. Use of two-phase loop thermosyphons for thermoelectric refrigeration: experiment and analysis. Appl Therm Eng 2003;23(9):1167–76.
[83] Vián JG, Astrain D. Development of a thermoelectric refrigerator with two-phase thermosyphons and capillary lift. Appl Therm Eng 2009;29(10): 1935–40.
[84] Omer SA, Riffat SB, Ma X. Experimental investigation of a thermoelectric refrigeration system employing a phase change material integrated with thermal diode (Thermosyphons). Renew Energy 2001;21:1265–71.
[85] Jugsujinda S, Vora-ud A, Seetawan T. Analyzing of Thermoelectric Refrigerator Performance. Procedia Eng 2011;8:154–9.
[86] Dai YJ, Wang RZ, Ni L. Experimental investigation and analysis on a thermo-electric refrigerator driven by solar cells. Sol Energy Mater Sol cells 2003;77:377–91.
[87] Riffat SB, Qiu G. Comparative investigation of thermoelectric air-conditioners versus vapour compression and absorption air-conditioners. Appl Therm Eng 2004;24(14–15):1979–93.
[88] Harman TC, Walsh MP, Laforge BE, Turner GW. Nanostructured thermoelectric materials. J Electron Mater 2005;34(5):19–22.
[89] Oró E, de Gracia A, Castell A, Farid MM, Cabeza LF. Review on phase change materials (PCMs) for cold thermal energy storage applications. Appl Energy 2012;99:513–33.
[90] Sechilariu M, Wang B, Locment F. Building-integrated microgrid: Advanced local energy management for forthcoming smart power grid communication. Energy Build 2013;59:236–43.
[91] Yan J, Chou SK, Desideri U, Tu ST, Jin HG. Research, development and innovations for sustainable future energy systems. Appl Energy 2013;112: 393–5.